

UDC 622.25

**M. S. PLESHKO**<sup>1,2</sup>, Professor, Doctor of Engineering Sciences, [mixail-stepan@mail.ru](mailto:mixail-stepan@mail.ru)  
**A. N. PANKRATENKO**<sup>1</sup>, Head of Department, Professor, Doctor of Engineering Sciences  
**A. A. NASONOV**<sup>3</sup>, Associate Professor, Candidate of Engineering Sciences  
**A. S. ISAEV**<sup>4</sup>, Chief Executive Officer, Candidate of Engineering Sciences

<sup>1</sup> National University of Science and Technology—MISIS, Moscow, Russia

<sup>2</sup> Don State Technical University, Rostov-on-Don, Russia

<sup>3</sup> Platov South-Russian State Polytechnic University (NPI), Novocherkassk, Russia

<sup>4</sup> Management Company ELSI LLC, Yakutia, Russia

## GEOMECHANICAL MONITORING AND STRESS–STRAIN ANALYSIS OF LINING IN ULTRA DEEP MINE SHAFTS

### Introduction

Large-scale mining is associated with a persistent increase in the mining depth. More than 20 mines in the world (South Africa, Canada, United States, India and Brazil) operate at depths greater than 2000 m. South African's biggest gold project—Mponeng Gold Mine has intersected the horizon at the depth of 4000 m below the surface of the earth.

Access to the super deeply buried ore bodies is attained via vertical shafts. Such shafts experience very high static and dynamic stresses. For example, in Tau Tona Mine, at a depth of 4000 m, the vertical stresses are 100 MPa. The deviation of the maximum principal stress direction from vertical makes 0–20° to NNW at a gradient of  $27 \pm 0.3$  MPa/km [1].

Regarding Russia, the actual depths of mining range from 700–900 m on the Kola Peninsula, to 1200 m in the Urals, and to more than 1000 m in Yakutia and in the Donets Basin [2, 3]. Skalisty Mine in the Norilsk Region is finishing construction of vertical shafts more than 2050 m deep. The construction has already taken 10 years and is planned to be completed by 2022.

Higher confining pressure induces stronger dynamic phenomena with an increasing depth, which complicates shaft sinking at Skalisty Mine and initiates hazardous geotechnical situations. The nature and mode of the phenomena of rock pressure are governed by natural factors and by the technology selected for shaft sinking. Another complicating factor is the lack of accurate and sufficient geological information on the properties and behavior of rock mass at depths more than 1500 m below ground surface.

In actual practice, such information can be obtained during field research into the stress–strain behavior of the shaft lining–rock mass system. Such research allows qualitative and quantitative estimation of geomechanical processes in the system and enables reliable determination of the load-bearing capacity margin of the lining in the period of shaft construction and operation [4, 5].

A detailed review of underground monitoring techniques and their application in Russia was given by [6]. The foreign research findings on the issue is presented in [7–18].

The regular and full-scale studies of mine shafts were put into practice in the 1950s in Russia. The measuring tools were dynamometric pressure vessels, pressure transducers, extensometers and wire strain gauges. The measuring equipment using these tools was only applicable to a depth of 1100 m in mine shafts in Russia.

Recently, the building and construction sectors boost introduction of fibre-optic sensing-based monitoring. Fibre optics is advantageous over

*Currently Skalisty Mine in the Norilsk Region of Russia is finishing construction of two vertical shafts 2050 m deep in very difficult geological and climatic conditions. This study uses the geotechnical monitoring data on one shaft and the stage-wise numerical modeling results to reveal mechanisms of stresses in the shaft lining and to assess efficiency of technologies and designs in use. It was found that high stress relaxation took place in the region around the shaft before installation of permanent support. The measured normal and shear stresses in shotcrete lining exceeded the calculated values, and the asymmetry of the stresses was observed in the cross-section of the shaft. Regarding the permanent support, the measured maximal compressive stresses were lower than the calculation. The analysis confirms the ultra deep shaft stability. The assumed designs and technologies for the ultra deep shaft construction are optimal.*

**Keywords:** Mine shaft, lining, rock mass, monitoring, numerical modeling, stresses, displacements, concrete, strength

**DOI:** 10.17580/em.2023.01.03

traditional sensors for: small size and weight; embeddability in the test material; fire- and explosion-safety; electromagnetic immunity; high corrosion, chemical and radiation resistance; high accuracy; distributed measurability; high-rate response to change in the quantity to be measured.

However, in Russia, there are no approved techniques for geotechnical monitoring of mine shafts using fibre-optic sensing thus far, while the component parts of these systems are very expensive.

All things concerned, development and introduction of efficient geomechanical monitoring of shaft lining–rock mass system in super deep mine shafts is of high relevance in Russia.

This paper aims to provide a comprehensive overview of geomechanical monitoring and mathematical modeling accomplished in Skalisty Mine, in mine shaft SKS-1, at its bottom, in the depth interval between 1800 and 2050 m, including a few mine roadways in the near wellbore region, the presence of which even more complicates the geomechanical situation. The authors discuss selection of an efficient technology for shaft sinking and an appropriate design of lining, and compare the modeling and actual monitoring results. Section 2 of this paper offers a brief review of engineering data and geological conditions of the shaft in the test area. Then, the numerical model of the shaft and the approaches to modeling are described. Some theoretical and practical aspects of monitoring are addressed in Section 4. Finally, the research findings are analyzed, and recommendations are given for the further investigation.

### Shaft sinking technology and conditions

Skip and cage shaft SKS-1 having a bore diameter of 9.0 m and a depth of 2050.5 m is intended for the transport of personnel and cargos, for ore hoisting to ground surface and to supply fresh air in the mine.

**Table 1. Physical and mechanical properties of rocks**

Type of rocks	Reduced Young's modulus with regard to rock mass quality, E, GPa	Poisson's ratio $\mu$	Density $\gamma$ , t/m <sup>3</sup>	Compressive strength*, MPa	Tensile strength, MPa	Internal friction angle $\varphi$ , deg	Cohesion C, MPa
1. Porphyritic basalt, diabase, calciferous mudstone, dolomite, limestone	25	0.27	2.75	120–180	8–14	40–50	14–24
2. Sandstone, anhydrite–carbonate rocks	21	0.26	2.7	120–160	8–12	35–45	12–18
3. Reddish-brown mudstone (including brownish-purple)	26	0.21–0.25	2.8	140–160	11–28	36–40	26
4. Anhydrite	32	0.22–0.27	2.7	108–180	12–14	40–50	13–18
5. Gabbro-dolerite (including fine-grained)	40	0.25	2.8	130–180	17–28	35–50	22–32
6. Greenish-grey, grey hornstone	31	0.22–0.24	2.75	120–170	15–30	38–42	20–32

\* marks the triaxial compressive strength

The shaft construction site is situated in the south-east of the Kharaelakh plateau, at the bottom of the western shoulder of the Skalistaya Mountain. This area features the severe dry continental climate, with negative average annual temperature and with long, heavily frosty and snowstormy winter.

The key geomechanical features of this shaft sinking include:

- High horizontal stresses comparable with and exceeding the uniaxial compression strength of rock mass;
- High-level faulting, especially nearby the Norilsk–Kharaelakh fault;
- Predominantly extensional tectonics in the form of reverse faults, dip-slips and strike-slips;
- Rockburst hazardous sulphide and copper ore, as well as enclosing rock mass in the field of Skalisty Mine.

**Table 1** gives the data on the physical and mechanical properties of jointed rock mass at depths greater than 1500 m.

Stresses are assessed using a tectonic geomechanical model. The principal stresses change almost linearly with depth of the shaft, and the maximal horizontal principal stresses  $\sigma_{hmax}$  are oriented along the normal to the Norilsk–Kharaelakh fault.

Considering high intensity of the horizontal stresses at great depths and aimed at advanced stress relaxation, it was decided to adopt SKS-1 shaft sinking technology with lagged installation of permanent support relative to the bottom face of the shaft (this is a parallel process flow chart as per the mining terminology assumed in Russia). The temporary support for the bottom face zone combined rock bolting, steel wire and shotcrete. At the depths of 1800–2050 m, it was decided to use steel and glass fibre reinforced polymer (GFRP) bolts having the length  $L = 3.0$  m, diameter  $D = 25.0$  mm and the resistance to rupture  $F = 340.0$  kN at the bolt density  $N_{bolt} = 1.0$  bolt/m<sup>2</sup>.

**Table 2** characterizes shotcrete lining and permanent concrete lining in the shaft.

**Algorithm for numerical modeling of vertical shaft**

For the stress–strain analysis and for the evaluation of the sinking technology effect on the stresses in the shaft under construction, 3D numerical models were developed and a series of stage-wise computations was implemented in MIDAS GTS NX environment. The stages of the numerical modeling include [19]:

1. Geometric simulation. The model at a scale of 1:1 has a prismatic shape. Aimed to avoid the influence of the boundary conditions,

**Table 2. Characteristics of shaft lining**

Characteristics	Shotcrete lining	Permanent concrete lining
Thickness, mm	200.00	500.00
Estimated strength, MPa	14.50	17.00
Deformation modulus, MPa	10700.00	11600.00
Poisson's ratio	0.21	0.21
Lagging of lining relative to shaft bottom face before a new sinking cycle, m	8.00	28.00

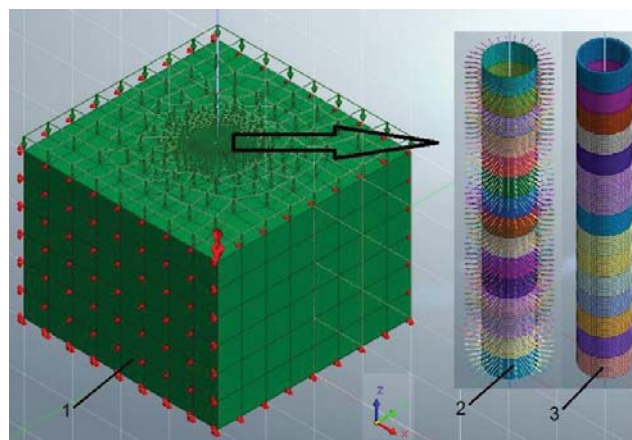


**Fig. 1. Finite element model of shaft:**  
1–general view; 2–bolting+shotcreting; 3–permanent support

the horizontal dimension of a face is assumed as 80.0 m, which exceeds 10 diameters of the shaft. The height of the model is 60.0 m (**Fig. 1**).

2. Setting of properties of rocks and support materials. The Mohr–Coulomb model is assumed for the rock mass deformation, as consistent with the properties of rocks in Table 1. For the materials of lining, an elastic model is adopted.

3. Selection of finite elements. It is chosen that rocks and lining are represented by 3D isoparametric 6-point and 8-point finite elements (three- and four-sided prisms with nodes at points of finite elements). Shotcrete lining is given as flat finite elements as an envelope of a constant thickness, and rock bolts are represented by rod finite elements.

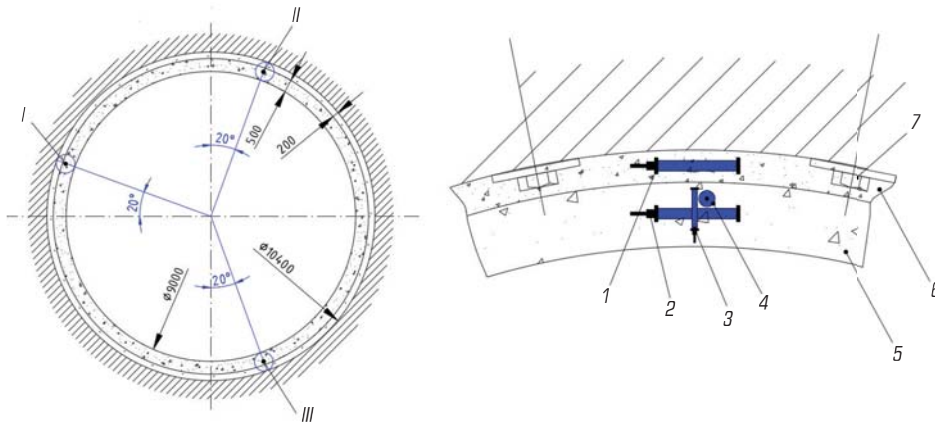


**Fig. 2. Layout of strain sensors in shaft cross-section:**  
 I, II, III—groups of sensors; 1—tangentially oriented sensors in shotcrete lining; 2, 3 and 4—tangentially, radially and vertically oriented sensors in permanent lining; 5—permanent lining; 6—advanced temporary shotcrete lining; 7—rock bolts

4. Mesh generation. The mesh density is assumed as 0.25 m inside the computational domain and up to 10.0 m at the external boundaries of the model (Fig. 2). In the shaft interval 60.0 m long, 15 entry ways 4.0 m long are identified. Finite elements are generated for rocks, bolts, shotcrete lining and concrete lining in entry way.

5. Setting of boundary conditions. The boundary conditions are set as limited normal displacements of the sides and bottom of the model.

6. Setting of loads. The model includes own weights of all elements. Furthermore, the model is subjected to the tectonic stress field depicted by the curves in Fig. 1.

7. Identification of computation phases. The initial phase includes all elements of rock mass and isolates all elements of lining. It is set that the vertical strains are zeroed after accomplishment of the initial phase. The loads from the lining, own weight and tectonic stresses are incorporated in the initial phase. Thus, the initial phase conforms with the natural condition of rock mass before sinking is started. Then, modelling represents the successive stages of the shaft sinking by cuts 4.0 m long, with gradual inclusion of the elements of the temporary and permanent lining. Rock bolts in a cut (a pattern of 4 rows at a preset density) is included at the second step, after exclusion of the finite elements of the second cut on the bottom face; the shotcrete lining is included at a lag of two cuts; the permanent lining is included at a lag of seven cuts. All in all, there are 22 computation steps; at the final step, we have a complete model of a driven and supported shaft interval 60.0 m long.

8. Calculation and analysis. The phase-by-phase computation allows the stage-wise analysis of the shaft construction. The stresses determined in the initial phase are added to the elements engaged in the next phases as contact stresses. As a result, displacement of the model points, as well as the forces and stresses in the rod, flat and 3D finite elements are determined in each computation phase. The principal and equivalent stresses are calculated, and the inelastic strain zones are delineated.

**Shaft monitoring procedure**

Geotechnical monitoring can help determine some parameters of the stress–strain behavior of lining and adjacent rock mass: displacements, relative strains, stresses, etc.

The geotechnical monitoring program developed and implemented for integrated sinking and construction safety in SKS-1 shaft includes:

1. Advanced exploration drilling from the shaft bottom face, adjustment of actual structure and properties of enclosing rock mass;

2. Determination of shaft convergence;  
 3. Measurement of relative shear strains in temporary shotcrete lining;

4. Measurement of relative shear, vertical and radial strains in permanent concrete lining.

The convergence measurements used Geokon’s 1610s tape extensometers having an error of ±0.01 mm.

Four rod extensometers were installed in the shaft walls at a distance of 1 m from the bottom face. As a result, two measurement axes were formed, which passed through the center of the shaft cross-section, in the directions of the effective maximal and minimal principal horizontal stresses in rock mass. The distance between the extensometers was measured:

- In the beginning of sinking, before starting drilling-and-blasting;
- After blasting, during mucking;
- On the lower level of the sinking platform after advance of the bottom face;
- On the second level of the sinking platform, prior to the permanent support installation at the level of the extensometer.

The convergence was evaluated as the difference between the initial distance  $D_0$  between the sensors at a temperature  $T_0$  and the subsequent distance  $D_i$  at a temperature  $T_i$ ;

$$\Delta D = D_i - D_0 + D_0 K (T_i - T_0), \tag{1}$$

where  $K$  is the thermal expansion coefficient of the extensometer tape,  $K = 11.6 \cdot 10^{-6} \text{ m/m}^\circ\text{C}$ .

Relative strains in the lining during sinking were determined using four sensing stations composed of sensors, communications and data collectors.

Each sensing station included three groups of different type sensors arranged at different cross-section points of the shaft (see Fig. 2). Sensors of type 1 (Fig. 3) were set at the shaft bottom before shotcreting. Sensors of types 2–4 were installed from the sinking platform before application of the permanent concrete lining.

The first type sensors installed in the advanced shotcrete lining measured tangential deformation. The sensors of the other three types measured deformation along all spatial axes in the permanent concrete support (see Fig. 3).

The specifications of the sensors are collected in Table 3.

The relative strain is given by:

$$\varepsilon = \Delta/L, \tag{2}$$

where  $\Delta$  is the absolute variation in spacing of sensors along the principal axis, mm;  $L$  is the initial spacing of sensors (sensor gauge length), mm.

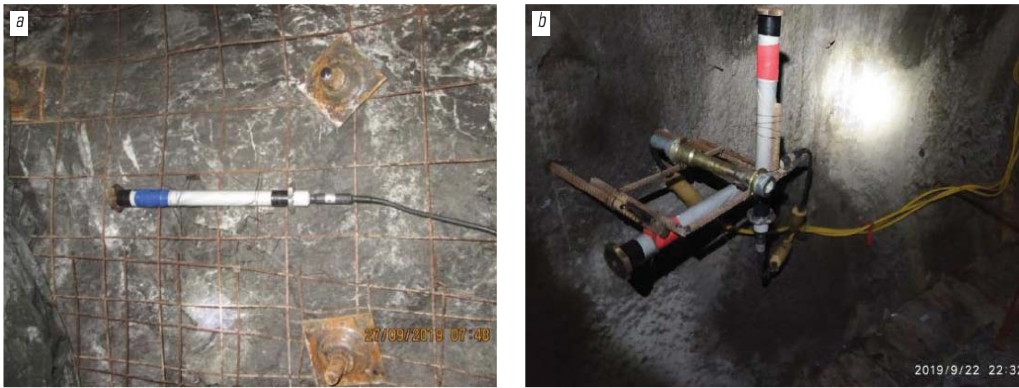


**Fig. 3. Sensors installed in shaft:** before shotcreting (a); before application of permanent concrete lining (b)

**Table 3. Specifications of sensors**

Description	Sensor		
	PLDS-M-400S	PLDS-M-400R	TB-200
Orientation, installation site	Tangential, temporary and permanent support	Vertical, permanent support	Radial, permanent support
Compressive strain limit, 1/mln	2000	500	1600
Tensile strain limit, 1/mln	500	2000	500
Measurement range, mm	400	400	200
Basic error	±2.0%	±2.0%	±1.0%
Range of operating temperatures	-30...+40°C	-30...+40°C	-30...+50°C
Limiting pressure, MPa	3.0	3.0	2.0
Sensor diameter, mm	65	65	60
Cable-free length, mm	530	530	320
Weight, kg	2.5	2.5	1.5
Service life, years	14	14	20

The strain to be measured is related with an outlet signal cycle of each specific sensor as follows:

$$\epsilon = A/x^2 - B/X + C, \quad (3)$$

where  $\epsilon$  is the measured strain, mln<sup>-1</sup>;  $X$  is the cycle of an outlet signal,  $\mu$ s;  $A$ ,  $B$ ,  $C$  are the constants determined from calibration tests of the sensors, mln<sup>-1</sup>· $\mu$ s<sup>2</sup>, mln<sup>-1</sup>· $\mu$ s, mln<sup>-1</sup> respectively.

The relation of the temperature and electrical resistance of the coil block is individual for each sensor and is given by:

$$T = G \cdot R + H, \quad (4)$$

where:  $T$  is the ambient temperature at the sensor, °C;  $R$  is the DC resistance of copper wire coil of transducer mount, Ohm;  $G$  and  $H$  are the constant coefficients determined from calibration tests of a specific sensor, °C/Ohm, °C.

All in all, over the period from 19 June 2019 to 15 December 2019, four measurement stations were installed in SKS-1 shaft and correlated with representative layers in the geological section. The monitoring data are discussed and compared with the numerical modelling results in Section 4 of this paper. For the convenience of the data representation, the compressive stresses and strains are assumed to be positive, and the tensile stresses are strains—negative.

**Table 4. Stresses in shotcrete lining of shaft**

Measurement station No.	Depth $H$ , m	Uniaxial compression strength, MPa	Calculated normal and shear stresses, MPa	Measured normal and shear stresses, MPa
1a	1957.7	51.4	9.79	11.0
2a	1977.0	50.2	16.31	19.8
3a	2007.8	42.1	13.28	15.1
4a	2024.0	33.2	17.13	18.04

**Table 5. Stresses in permanent concrete lining of shaft**

Measurement station No.	Depth $H$ , m	Uniaxial compression strength, MPa	Calculated stresses, MPa			Measured maximal stresses, MPa		
			$\sigma_1$	$\sigma_3$	$\sigma_3$	$\sigma_1$	$\sigma_3$	$\sigma_3$
1b	1936.8	42.0	2.90	1.34	-0.12	2.2	1.2	-0.2
2b	1981.8	54.0	4.12	1.44	-1.23	3.9	1.6	-1.6
3b	1999.8	67.5	4.20	1.36	-0.78	3.1	1.4	-0.9
4b	2026.5	44.9	3.86	1.25	-0.67	1.3	1.1	-1.0

**Numerical modeling and geotechnical monitoring results: Analysis and comparison**

The process of rock mass deformation in the course of shaft sinking can be divided into some major stages:

1. Deformation after exposure up to installation and actuation of temporary lining;
2. Joint rock mass—temporary lining deformation;
3. Deformation of rocks after installation and actuation of permanent support until static equilibrium in the rock mass—lining system.

The research data on these stages in the first test site are discussed below. The experimental results are also compared with the calculations. The location depths of the measurement stations are given in **Tables 4** and **5** for the shotcrete lining and permanent concrete lining, respectively. Convergence of the shaft at the bottom face was studied at these depths.

The convergence is depicted as a function of distance to the shaft bottom in **Fig. 4**. Each point in the plot is an averaged value of four measurements.

The modeling results in the form of isofields of horizontal displacements in the first test site in the bottomhole zone of the shaft are demonstrated in **Fig. 5**.

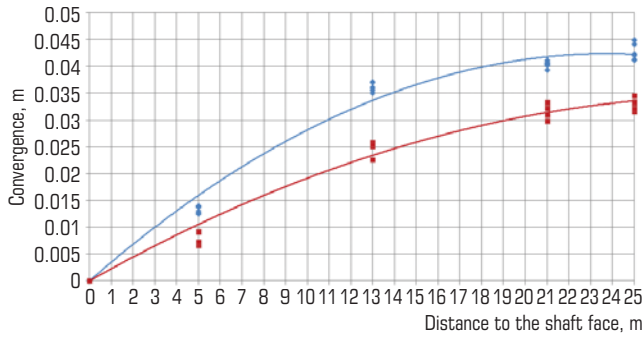


**Fig. 4. Shaft convergence along mutually perpendicular axes of shaft cross-section (first test site, location depth of sensors—1957.7 m)**

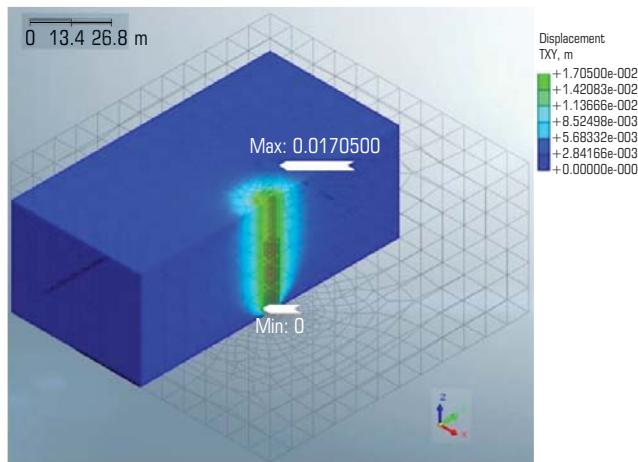


**Fig. 5. Isofields and values of radial displacements in model shaft**

The comparison of the modeling and in-situ tests shows that before installation of the permanent support, the substantial relaxation of stresses takes place in rock mass which deforms jointly with shotcrete and bolts. The calculated convergence in four test sites is 15–20% less than the field measurements. This can be explained by the effect of rock mass fracturing in real life, and by the larger actual diameter of the shaft as against the project value. On the whole, during the monitoring period, no rock falls, or excessive strains in the temporary lining, fracturing or shear failure of rock bolts were observed.

The time history of relative deformation in the shotcrete and permanent concrete lining in the first test site of the shaft is demonstrated in **Fig. 6**.

The analysis of the monitoring data shows two stages of heavy loading applied to the shotcrete lining. The first stage is the early period of 20 days when the shotcrete lining develops its strength, comes into play and takes on ground pressure during further sinking.

The second stage begins after installation and actuation of the permanent shaft support. Shotcrete as an interlayer works in the condition of triaxial compression. Moreover, temperature strains arise due to heat inflow from solidifying concrete of the permanent lining. Then, strains stabilize, and stress asymmetry is observed in the lining in the cross-section.

The analysis of the charts of the relative strain behavior in the permanent lining shows that the process stabilizes after completion of

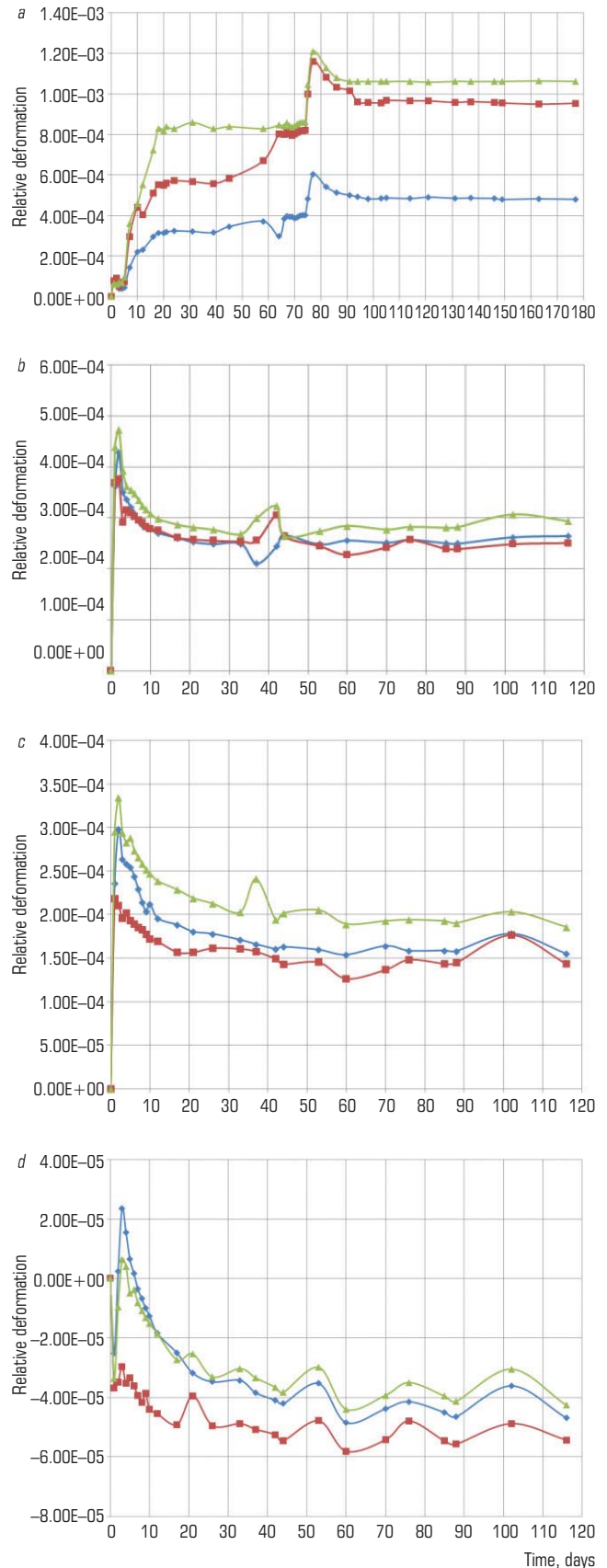


**Fig. 6. Time history of relative deformation in shaft lining: tangential strains in shotcrete (a); tangential strains in mass concrete (b); vertical strains in mass concrete (c); radial strains in mass concrete (d)**

active phase in concrete curing (5 days). The peaks of strains in this phase are governed by heating of concrete in curing. The similarity of the charts and the low levels of strains are indicative of the normal operating mode of the permanent support. The temperatures and shrinkage strains settle finally 10–15 days after concrete casting. Subsequent monitoring revealed no essential strain jumps in the permanent lining in any of four test sites.

Using the measured displacements, the maximal stresses are determined in the shotcrete and permanent lining and compared with the numerical modelling data in the test sites (Tables 4 and 5).

The comparative analysis of the results shows that the measured normal and shear stresses in shotcrete lining exceed the calculated values, which can be due to:

(a) the excess of the actual cross-section over the project cross-section of the shaft;

(b) the longer actual rock mass–shotcrete interaction prior to installation of permanent lining. For instance, at the depth of 1977 m, this period lasted for more than 60 days;

(c) the higher actual strength of shotcrete and thicker layer of lining, which resulted in a rigid and unyielding temporary support.

On the whole, the calculation and experiment agree well, at deviation not more than 22%.

Regarding the permanent lining, the measured stresses in the discussed period of observations are much less than the calculation. The support possesses high safety margin in all test sites of the shaft. The maximal difference between the calculated and measured stresses in the permanent support exceeds 60%. This is explained by the influence of many factors unintegratable completely in numerical modelling.

### Conclusions

This paper has presented a case-study of the stress–strain analysis of a deep vertical shaft in the period of sinking using experimental approaches and computational methods. The proposed procedure allows the shaft convergence evaluation, as well as the stress and displacement assessment in temporary and permanent lining, and enables a prompt adjustment of shaft support design with changing geomechanical situation.

In terms of SKS-1 shaft in Skalisty Mine, the preset process design and engineering solutions have proved to be effective as they ensure operating safety and high functional reliability of the shaft support at the initial stage of its interaction with adjacent rock mass. The new experience contradicts the common practice adopted in Russia and earlier in the former Soviet Union for the permanent lining installation right after bottom face advance in mine shaft sinking (a simultaneous flow chart). The latter flow chart was used in construction of more than 14 deep vertical shafts in Norilsk mines. During operation of the shafts, their lining suffered from considerable damages and deformation, which required expensive repair. Some researchers suppose that minimization of stresses in the permanent shaft support in case of consecutive sinking and lining in the conditions of the Norilsk industrial region will be of temporal nature and permanent lining will undergo increasingly higher loading with time. The most hazardous time span is the gradual efficiency loss in the bolting designed for the service for 15–20 years. Thus, it is very important to continue shaft monitoring during operation. In order to collect a representative data base on the same engineering facilities, it is expedient to introduce fibre-optic sensing systems in shafts, which is the subject of further research of the authors.

### References

- Corkum A. G., Damjanac B., Lam T. Variation of horizontal in situ stress with depth for long-term performance evaluation of the Deep Geological Repository project access shaft. *International Journal of Rock Mechanics and Mining Sciences*. 2018. Vol. 107. pp. 75–85.
- Kaledin O. S. Innovative construction technology for ultra deep shafts. *Gornyi Zhurnal*. 2014. No. 4. pp. 77–81.
- Zubkov A. V., Feklistov Yu. G., Sentyabov S. V. Special characteristics of stress-strain state development in a concrete support of Donskoy and Gaisky GOKs shafts. *Izvestiya vuzov. Gornyi zhurnal*. 2019. No. 4. pp. 12–23.
- Kharisov T. F. Mine shaft rock walls convergence investigations in the conditions of the out-of-limit state of the borehole massif. *Izvestiya vuzov. Gornyi zhurnal*. 2017. No. 5. pp. 46–51.
- Sentyabov S. V. Analysis and prediction of change in stress state of shaft lining in Gaisky mine. *GIAB*. 2018. No. 10. pp. 79–85.
- Kazikaev D. M., Sergeev S. V. Diagnostics and monitoring of stressed state of vertical shafts' timbering. Moscow : Gornaya kniga, 2011. 244 p.
- Lucier A. M., Zoback M. D., Heesakkers V., Reches Z., Murphy S. K. Constraining the far-field in situ stress state near a deep South African gold mine. *International Journal of Rock Mechanics and Mining Sciences*. 2009. Vol. 46, Iss. 3. pp. 555–567.
- Strickland B., Board M., Sturgis G., Berberick D. Elliptical shaft excavation in response to depth induced ground pressure. *The Future for Mining in a Data-Driven World : 2016 SME Annual Conference & Expo. Phoenix*, 2016.
- Walton G., Kim E., Sinha S., Sturgis G., Berberick D. Rock Mechanics Challenges for the Excavation of a Deep Shaft in Anisotropic Ground. *52<sup>nd</sup> U.S. Rock Mechanics. Geomechanics Symposium*. Seattle, 2018. Vol. 5. pp. 4031–4036.
- Weizhang Liang, Guoyan Zhao, Xi Wang, Jie Zhao, Chunde Ma. Assessing the rockburst risk for deep shafts via distance-based multi-criteria decision making approaches with hesitant fuzzy information. *Engineering Geology*. 2019. Vol. 260. 105211. DOI: 10.1016/j.enggeo.2019.105211
- Xiaowei Feng, Nong Zhang, Fei Xue. et al. Practices, experience, and lessons learned based on field observations of support failures in some Chinese coal mines. *International Journal of Rock Mechanics and Mining Sciences*. 2019. Vol. 123. 104097. DOI: 10.1016/j.ijrmm.2019.104097
- Han J.Y., Guo J., Jiang Y. S. Monitoring tunnel profile by means of multi-epoch dispersed 3D LiDAR point clouds. *Tunnelling and Underground Space Technology*. 2013. Vol. 33. pp. 186–192.
- Jones E., Beck D. The use of three-dimensional laser scanning for deformation monitoring in underground mines. 2017. Available at: <http://beckengineering.info/?p=2731> (accessed: 21.04.2022).
- Yun H. B., Park S. H., Mehdawi N., Mokhtari S., Chopra M. et al. Monitoring for close proximity tunneling effects on an existing tunnel using principal component analysis technique with limited sensor data. *Tunnelling and Underground Space Technology*. 2014. Vol. 43. pp. 398–412.
- Zhou H., Qu C.K., Hu D. W., Zhang C. Q., Azhar M. U. In situ monitoring of tunnel deformation evolutions from auxiliary tunnel in deep mine. *Engineering Geology*. 2017. Vol. 221. pp. 10–15.
- Di Murro V., Pelecanos L., Soga K., Kechavarzi C., Morton R. F., et al. Long term deformation monitoring of CERN concrete-lined tunnels using

- distributed fibre-optic sensing. *Geotechnical Engineering Journal of the SEAGS & AGSSEA*. 2019. Vol. 50, Iss. 2. pp. 1–7.
17. Forbes B., Vlachopoulos N., Hyett A. J. The application of distributed optical strain sensing to measure the strain distribution of ground support members. *FACETS*. 2018. Vol. 3, No. 1. pp. 195–226.
18. Klar A., Dromy I., Linker R. Monitoring tunneling induced ground displacements using distributed fibre-optic sensing. *Tunnelling and Underground Space Technology*. 2014. Vol. 40. pp. 141–150.
19. Pleshko M. S., Silchenko Yu. A., Pankratenko A. N. et al. Improvement of the analysis and calculation methods of mine shaft design. *GIAB*. 2019. No. 12. pp. 55–66. **EM**

UDK 622.832

**M. B. NURPEISOVA**<sup>1</sup>, Doctor of Engineering Sciences, Professor, marzhan-nurpeisova@rambler.ru**A. M. ABENOV**<sup>1</sup>, Doctoral student**N. A. MILETENKO**<sup>2</sup>, Senior Researcher, Candidate of Engineering Sciences**G. Zh. DOSETOVA**<sup>3</sup>, Candidate for a Doctor's Degree<sup>1</sup> K. I. Satpayev Kazakh National Technical University, Almaty, Kazakhstan<sup>2</sup> Academician Melnikov Research Institute of Comprehensive Exploitation of Mineral Resources–IPKON, Russian Academy of Sciences, Moscow, Russia<sup>3</sup> Abylkas Saginov Karaganda Technical University, Karaganda, Kazakhstan

## HIGHLY EFFICIENT MONITORING PROCEDURE FOR DEFORMATION PREDICTION IN COPPER ORE MINING

The Earth population grows yearly and is going to face the lack of mineral resources very soon. Mineral mining will be carried out in difficult geological conditions, at great depths, and with drastic environmental consequences [1].

In Kazakhstan, the mining sector is one of the most advanced job-offering industries. For the complete extraction of mineral raw materials, mining activities extensively involve mineral deposits at great depths in difficult ground. Naturally, major complications are expected due to geomechanics and geodynamics in this case. The geomechanical and geodynamic processes entail not only catastrophic technical and economic consequences, but sometimes lead to human casualties. Induced earthquakes occur in Germany, USA, Poland, Czech Republic. In Russia, this problem is critical in the mines of the Upper Kama potash salt deposit and the Khibiny apatite nepheline massif [2, 3]. All this is a direct consequence of geodynamic alteration of geological environment under the impact of large-scale mining, which is convincingly confirmed by the results of long-term scientific research of the Zhezkazgan nature-and-technology system, which is formed by mines, concentration factories with tailings and, copper smelters in Karaganda, Balkhash, Zhezkazgan and Satpaev. The mining infrastructure in Central Kazakhstan also exerts a powerful anthropogenic impact on the environment and offers comprehensive facilities to study a wide range of environmental problems [4–6].

*The new highly effective rock mass behavior monitoring procedure ensures environmental and industrial safety in the area of Central Kazakhstan. The implemented integrated research includes the analysis of the geology, structure and physical and mechanical properties of rocks mass, as well as in-situ monitoring using the authorial methods and means. The accomplished research results are: the geodynamic test ground; the designs of the permanent (surface and underground) forced centering points of enhanced capacity and accuracy, the method of 3D laser scanning of rock mass structure, which allows a comprehensive study of fractures and faults in rock mass, the stress–strain behavior prediction method, as well as the composition of a reinforcement solution made of mining waste to enhance stability of dislocated pitwall slopes.*

*The geodynamic test ground created for mineral deposits in Central Kazakhstan is a reliable framework for the long-term ground deformation monitoring in large-scale mineral mining at the enhanced capacity and accuracy of observation. The results are applicable in operating safety improvement and ecological risk minimization in underground mineral mining.*

**Keywords:** deposits, fracturing, rocks, physical and mechanical properties, stress state, mining, monitoring, geodynamic test ground, geodetic network, geodetic surveys, satellite systems, accuracy assessment  
Introduction

**DOI:** 10.17580/em.2023.01.04

### Literature review

The geomechanical studies were carried out in individual mines and promoted gain of experience in this area. The mining industry dynamics in Kazakhstan and in the world over the past century has led to a qualitatively new situation, when the 'local' geomechanical fields induced by anthropogenic activities are no longer small in comparison with the global geodynamic processes and tectonic activity of the Earth [7–9]. Consequently, it is necessary to consider mines as unique natural laboratories, where it is possible to study in detail the relationship of the geomechanical and geodynamic processes using geophysical and satellite geodetic methods [10, 11].